

FeGaB(25 nm)/Al₂O₃/FeGaB(25 nm) Multilayer Structures: Effects of Variation of Al₂O₃ Thickness on Static and Dynamic Magnetic Properties

Shahid Imran¹, Yin Ge², Yuan Jun², Ma Yungui², He Sailing^{1,2,3}

¹ ZJU-SCNU Joint Research Centre of Photonics, South China Normal University, Guangzhou 510006, China; ² State Key Laboratory of Modern Optical Instrumentation, Zhejiang University, Hangzhou 310058, China; ³ Royal Institute of Technology, S-100 44 Stockholm, Sweden

Abstract: Iron-gallium (FeGa) thin film has the unique advantages in designing integrated magnetic sensors or chips due to its relatively large magnetostrictive constant compared with other soft magnetic materials. In this work, non-magnetic doping and laminating methods have been employed to control the magnetic and electric properties of this alloy film. By doping a certain amount of boron (B), the coercivities are largely decreased for samples of thickness less than ~30 nm. For thicker films, we find that inserting an ultrathin Al₂O₃ middle layer is very helpful to control the coercivities with negligible influence on saturation magnetization (M_s). The smallest easy-axis coercivity of 0.98×79.6 A/m is obtained in the multilayer film FeGaB(25 nm)/Al₂O₃(0.5 nm)/FeGaB(25 nm). In this case, the resistivity is enhanced by 1.5 times compared with the 50 nm single layer film. Structural characterizations indicate the reductions of crystalline quality and physical dimension of the magnetic grains playing important roles in softening the magnetic properties. Besides, the influences of magnetostatic interaction and morphology characteristics are also considered in facilitating domain reversal. High permeability spectra with gigahertz response are obtained for our multilayer films. The methodology applied here, i.e., enhancing magnetic and electric performance by introducing ultrathin non-magnetic layers, could be translated to other species of soft magnetic materials as well.

Key words: iron-gallium boron; multilayer structure; aluminum oxide; soft magnetic property

Due to high values of magnetostriction as well as superior mechanical properties, FeGa thin films are widely investigated in the magnetic field for their potential applications as the key component in micro-and-nano electromechanical systems (MEMS/NEMS) [1], sensors [2,3] and actuators [4]. Soft magnetic properties of the cubic FeGa films critically depend upon the composition used. The pure binary alloy usually exhibits large coercivities due to its relatively high magnetocrystalline anisotropy [5]. It was found that good soft magnetic properties with coercivity less than 79.6 A/m for Fe₈₀Ga₂₀ magnetic films could be attained by doping a certain amount of boron [6]. This doping method for magnetic films using nonmagnetic elements like B, N, Si, etc. has been widely applied to improve the soft magnetic properties for various magnetic thin films [7-10]. However, it is

usually accompanied with undesired negative effects, for example, reducing saturation magnetization and magnetostriction constant if the doping concentration in the magnetic component is high. In practice, the dopant amount needs to be optimized to balance different magnetic parameters. On the other hand, a multilayering technique is also regarded as an efficient method to control the microstructures and properties of magnetic films without diluting [11-14]. For this purpose, nonmagnetic metallic or insulating materials as the spacing layer have been generally investigated in order to control both magnetic and electric properties [15-17]. So far the multilayer technique has been mainly conducted on iron [18,19], iron cobalt [20,21] or permalloy [11,22] based soft magnetic film systems. For example, Katori et al. [23] showed that not only better soft magnetic properties but also good thermal stability

Received date: July 13, 2017

Foundation item: National Natural Science Foundation of China (61271085, 91233208); Guangdong Innovative Research Team Program (201001D104799318)

Corresponding author: Ma Yungui, Ph. D., Professor, Center for Optical and Electromagnetic Research, College of Optical Science and Engineering, Zhejiang University, Hangzhou 310058, P. R. China, Tel: 0086-571-88206514-209, E-mail: yungui@zju.edu.cn

Copyright © 2018, Northwest Institute for Nonferrous Metal Research. Published by Elsevier BV. All rights reserved.

were attained for multilayered structure Fe-Al-N/Si-N and Naoe et al.^[22] reported 4×79.6 A/m coercivity value with Ni-Fe/Cu multilayered films.

In this work, we employ the advantages of both doping and laminating methods to optimize the soft magnetic properties and microwave performance of the FeGa thin films. Our discussion will be mainly focused on the laminating part as the doping one has been well addressed before^[6]. It is shown that different from the previous works^[24], a 0.5 nm Al₂O₃ insulating layer is necessary and enough to render the best soft magnetic properties with strong microwave permeability response. Structural characterizations reveal that the compositional and structural modifications could effectively suppress the crystallization and grain growth of the film, which make the films magnetically much softer by decreasing the magnetocrystalline anisotropy and raising the inter-grain exchanging coupling. Magnetostatic interaction and surface roughness are also considered to play positive roles in improving the soft magnetic properties. In addition, large damping factors are experimentally obtained from the fitting of the measured permeability spectra, which are understood in the background of multiple interaction forces in the composite systems.

1 Experiment

In this experiment, the sputtering system (Kurt Lusser, PVD 75) was used with two DC and two RF magnetron guns. The sputtering guns can accommodate 2-inch targets. The FeGaB films were sputtered on a single-crystal silicon substrate with (100) orientation from two separate targets of Fe₈₀Ga₂₀ (at%) and boron (B) using DC and RF magnetron guns simultaneously, while the Al₂O₃ films were deposited with the RF gun in the same sputtering system. The target powers of DC and RF guns were fixed to 30 and 60 W, respectively to obtain FeGaB films with sputter rate of 2.5 nm/min. A high resistivity silicon wafer ($>10000 \Omega\text{-cm}$) was selected as a substrate to avoid parasitic effects. Prior to deposition, silicon substrates were ultrasonically cleaned in acetone, methanol and 2-propanol, then rinsed in deionized water and dried under nitrogen (N₂) gas flow. To induce a uniaxial in-plane magnetic anisotropy in the FeGaB films, a static magnetic field of about 120×79.6 A/m was applied parallel to the surface of the films during deposition by placing permanent magnets across the substrates. Prior to deposition, all targets were cleaned for 5 min in a pure Ar atmosphere by keeping the shutter closed.

The thickness of the films was measured using a surface profilometer (Dektak 150) by generating a step using a shadow mask. FeGaB films were deposited with different thicknesses (25 and 50 nm) while the thickness of Al₂O₃ films varied between 0.5 nm and 12 nm at a rate of 0.66 nm/min keeping target power (80 W) fixed and increasing

the sputtered time. The structural properties were investigated with a Philips X-pert diffractometer using a Cu-K α line corresponding to a wavelength of 0.15406 nm. The surface topography was studied using an atomic force microscope (CSPM 5500). DC magnetic properties of single and multilayered magnetic films were recorded using a vibrating sample magnetometer (Lake Shore) at room temperature and static magnetic properties were determined from the hysteresis loops. The standard four-point measurement technique was used to measure the resistivity at room temperature. A vector network analyzer (Rohde & Schwarz, ZVA-40) was used to measure the microwave permeability at frequencies ranging from 0.5 to 4 GHz using a shorten microstrip transmission-line perturbation method^[25].

2 Results and Discussion

The binary Fe₈₀Ga₂₀ magnetic thin film we deposited shows very large coercivity $H_{ce} = 85 \times 79.6$ A/m with saturation magnetization $4\pi M_s = 1.64$ T. Boron doping was first conducted by tuning the sputtering gun powers: the power for FeGa target is fixed at 30 W and that for B target is varied from 60 W to 100 W. Higher sputtering power will increase the boron concentration in the film. The measured hysteresis loops show that the in-plane coercivity of the doped film decreases monotonously from 24.76×79.6 A/m to 3.56×79.6 A/m as the gun power of boron target increases from 60 W to 100 W, while the opposite trend is observed for the saturation magnetization that declines from 1.64 T to 1.39 T. The measured resistivity has slight variation around 200 $\mu\Omega\text{-cm}$. These results are consistent with the previously reported work^[6]. Boron dopant is expected to distribute around the boundary of grains and suppress their growth. The finer the average grain size $\langle D \rangle$ is, the stronger the exchange coupling between grains will be^[26]. Very good soft magnetic properties could be induced if the average grain size $\langle D \rangle$ becomes much smaller than the exchange coupling length or domain wall width. For the lamination processed below, we will start at a relatively high boron concentration with the sputtering power fixed at 60 W. This corresponds to $H_{ce} = 24.76 \times 79.6$ A/m and $4\pi M_s = 1.57$ T for 50 nm FeGaB single layer. We will show that the multilayer technique could be tailored to have good soft magnetic properties together with the additional advantages of less effect on M_s and high increase on electric resistivity. These parameters are vital for high-frequency inductive applications.

Before laminating, it is necessary to check how the film properties change with film thickness. Figs.1a and 1b plot the magnetic hysteresis loops of a 50 and 25 nm thick single layer FeGaB films, respectively. The easy (solid line) and hard (dotted line) axis loops are measured with the measuring field parallel and orthogonal to the external magnetic field applied during the film deposition that was

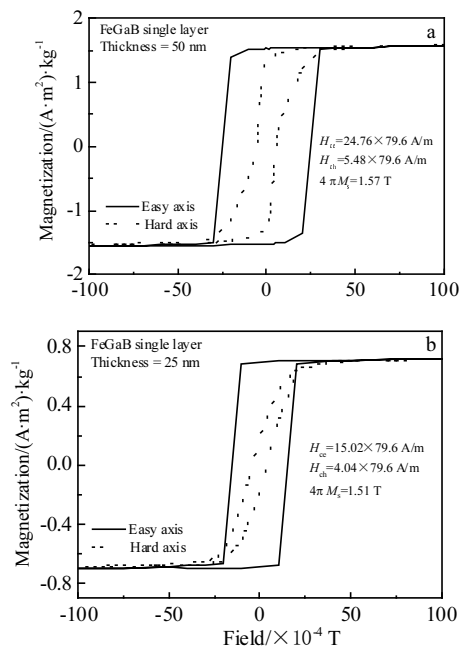


Fig.1 Hysteresis loops of FeGaB single layer film with different thicknesses (measured along easy or hard axis): (a) 50 nm and (b) 25 nm (the easy and hard axis coercivities and the saturation magnetization are given in the figures)

used to induce an extrinsic anisotropy, respectively. The loops show that the 25 nm thick film has well-defined uniaxial anisotropy compared to the 50 nm one and the anisotropy field H_k estimated from the hard-axis loop is about 20×79.6 A/m. When the thickness increases to 50 nm, the hysteresis loops become much broader and the coercivities increase significantly.

In this case, the inhomogeneous hard-axis loop indicates a mixed demagnetization process including domain rotation and wall motion as the uniaxial properties get worse. The saturation magnetization shows slight decrease (1.57 T \rightarrow 1.51 T) as the film thickness decrease from 50 nm to 25 nm, which may be explained by two reasons: (i) the structural quality (such as continuity) of the film is reduced when it becomes thinner, and (ii) a boundary diffusion layer of lower M_s may exist between the film and substrate^[27]. These assumptions are consistent with the measured resistivity that increases from 195 $\mu\Omega\cdot\text{cm}$ to 295 $\mu\Omega\cdot\text{cm}$ as the film thickness decrease. Figs.2a and 2b show the XRD patterns of the 50 and 25 nm FeGaB films, respectively. The crystallographic texture (110) is clearly observed for the thicker film, while it disappears for the thinner film. It means the thinner film has a lower crystalline degree and thus a weakened magnetocrystalline anisotropy, which is helpful to raise the soft magnetic properties. The same observation was detected for different ferromagnetic magnetic thin film systems below a certain value of film

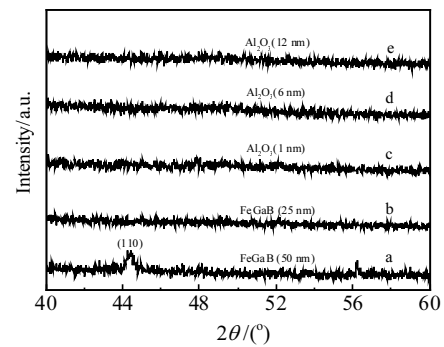


Fig.2 XRD patterns obtained for FeGaB single layer with thicknesses 50 and 25 nm and FeGaB(25 nm)/Al₂O₃/FeGaB(25 nm) sandwich structure with Al₂O₃ thickness of 1, 6 and 12 nm

thickness^[28]. Other issues like stress accumulation in thicker films may be also involved in degrading the soft magnetic properties^[29].

Further experiments show that the soft magnetic properties of the single layer film deflect at the film thickness of about 25~35 nm. In the following, we try to acquire good soft magnetic properties in the 50 nm FeGaB film through sandwiching it with an alumina interlayer while keeping the thickness of the magnetic sub-layer unchanged, i.e., a multilayer: FeGaB(25nm)/Al₂O₃(x)/FeGaB(25 nm) where x is the thickness of the oxide layer.

Fig.3 shows the in-plane easy-axis and hard-axis coercivities of the FeGaB(25 nm)/Al₂O₃(x)/FeGaB(25 nm) film as the function of the Al₂O₃ thickness ($x = 0.5\sim 12$ nm). The inset plots the hysteresis loops for the multilayered structures with Al₂O₃ layer. Alumina is selected here because it is insulating and could relatively easy to form smooth morphology at very small thickness. The low deposition yield for Al₂O₃ also helps to accurately control the thickness. From the curves, it is seen that the

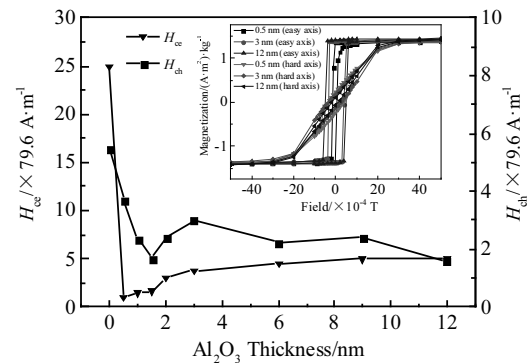


Fig.3 In-plane coercivity along the easy (H_{cc}) or hard axis (H_{ch}) as a function of the insulating layer thickness (the inset gives the magnetic hysteresis loops for multilayered structures with Al₂O₃ thicknesses of 0.5, 3 and 12 nm)

coercivities are obviously decreased once the oxide layer is introduced, in particular at $x = 0.5$ nm where a very small easy-axis coercivity $H_{ce} = 0.98 \times 79.6$ A/m is obtained. This result has been repeated twice. As the thickness increases from 0.5 nm to 9 nm, the easy-axis coercivity increases up to a value of 5×79.6 A/m and becomes constant for further increase of the insulating layer thickness. The hard-axis coercivity decreases from 5.48×79.6 A/m and remains steady between 4×79.6 A/m to 1.58×79.6 A/m for all variations of the Al_2O_3 thicknesses. Well-defined uniaxial anisotropy is observed for the multilayer films as shown in the inset loop figures. The anisotropy field has no obvious change remaining at about 22×79.6 A/m, mainly decided by the 120×79.6 A/m external field applied in the film deposition. As shown in Figs. 2c~2e, all the multilayer films have no obvious XRD peak, similarly indicating low crystalline quality. This could explain that the thin alumina alien layer effectively disrupts the continuous growth of the magnetic grains. Degradation of crystalline quality is expected to be a major reason for the reduction of coercivities observed in our multilayer films. Grain size reduction would be another reason in inducing the desired soft magnetic properties.

With further increase of Al_2O_3 thickness, the interface roughness may change, which is also the source of degradation of soft magnetic properties^[30]. To investigate this, surface topography observation of the samples Si/FeGaB(25 nm)/ Al_2O_3 (0.5~12 nm) was carried out with the help of AFM. The scan size was $1 \mu\text{m} \times 1 \mu\text{m}$ and the images were captured in non-contact mode. The three-dimensional (3D) AFM images for the samples of 0.5 and 12 nm alumina layers are given in Figs. 4a and 4b that show as the oxide layer gets thicker, the root mean square roughness (r_{ms}) value increases from 0.25 ± 0.05 nm to 1.17 ± 0.08 nm. Rougher surface will increase the density of the pinning sites that inhibit the domain reversal. This could explain the degradation of soft magnetic properties for the samples of thicker alumina layer, as shown in Fig. 3. In addition, the two isolated magnetic layers will interact with each other through the long-range magnetostatic interaction that will help to enhance the collective behavior in the domain demagnetization. But with the increase of the insulating layer thickness, this interaction will be weakened, which may also explain the slight increase of coercivities at larger x .

Figs. 5a~5d show the AFM images of the multilayer structure FeGaB/ $\text{Al}_2\text{O}_3(x)$ /FeGaB with $x = 0.5, 3, 12$ nm as well as single layer FeGaB with thickness 50 nm, respectively. Using the line scans across the morphology pictures, the average grain diameter for the multilayer structure is estimated between 26~28 nm, which is much smaller than that (40 nm) of the 50 nm single layer FeGaB film. The grain growth control is responsible for the reduction of coercivities. For the FeGa based films, the exchange coupling length L_{ex} , that defines the spatial scale

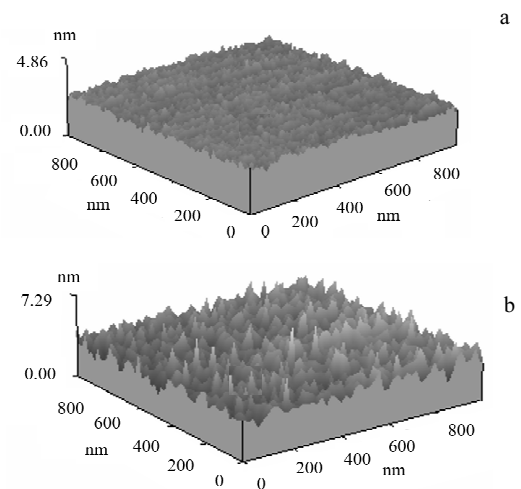


Fig. 4 3D AFM images of the multilayer structure FeGaB(25 nm)/ Al_2O_3 with Al_2O_3 thickness of 0.5 nm (a) and 12 nm (b)

within which we may expect a single domain behavior, is estimated to be ~ 92 nm using the relation^[31] below:

$$L_{ex} = \sqrt{A/K_1} \quad (1)$$

where the exchange stiffness $A = 1 \times 10^{-1} \text{ J}\cdot\text{m}^{-1}$ for FeGa^[32] and the magnetocrystalline anisotropy constant K_1 is calculated using the relation for FeGa^[33]:

$$K_1 = (M_s \times H_k) / 2 \quad (2)$$

The values of M_s and H_k are taken from the multilayer film with 0.5 nm thick Al_2O_3 . Since the average grain size of the multilayer films is much smaller than the exchange length, the inter-grain collective interaction within the magnetic sub-layer will be greatly enhanced assisted by the short-range exchange coupling force. As a result, the magnetic film will become softer. In addition, from the XRD peak shown in Fig. 2a, the Scherrer formula could give us another rough estimation on the average grain size ~ 20 nm for the 50 nm single layer FeGaB film. This value is much smaller than that evaluated from the AFM scanning. The difference may explain in the single layer film that there exists strong residual strain which further broadens the XRD peak^[34]. The sandwich structure with discontinuous film growth is helpful in controlling the residual strain in thick films, which is of benefit to the soft magnetic properties.

Table 1 lists the values of the saturation magnetization, anisotropy field as well as the resistivity on the thickness of the sample. The $4\pi M_s$ value fluctuates between 1.429 and 1.473 T. In our calculation, the volume of the nonmagnetic oxide layer is not considered. Opposite to the purely doping method, the laminating method could optimize the soft magnetic properties without sacrificing the largest available magnetization. But we may expect that there might exist mild diffusion at the interfaces that reduces the saturation magnetization^[17]. For the film of 0.5

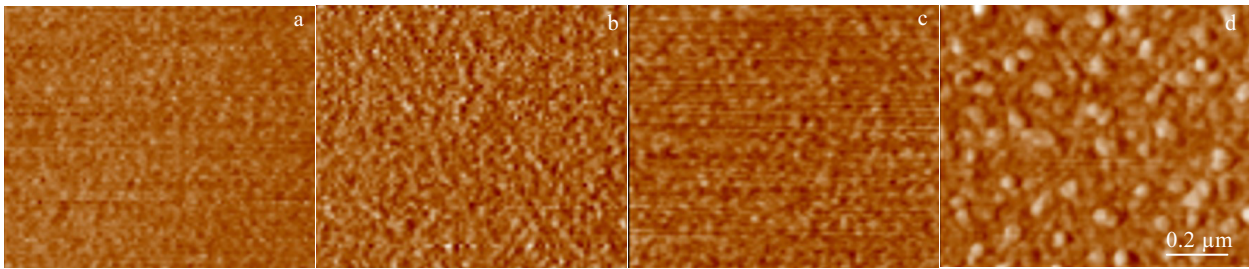


Fig.5 2D AFM images for the single and multilayer structures with different Al₂O₃ thickness: (a) 0.5 nm, (b) 3 nm, and (c) 12 nm; (d) single layer with 50 nm

Table 1 Saturation magnetization $4\pi M_s$, anisotropy field H_k , electrical resistivity ρ , calculated $f_{r,cal}$ using M_s and H_k , fitted initial permeability μ_i and damping factor α at different Al₂O₃ thickness

Al ₂ O ₃ thickness, x/nm	Saturation magnetization, $4\pi M_s /T$	Anisotropy field, $H_k/\times 79.6 A \cdot m^{-1}$	Resistivity, $\rho/\mu\Omega \cdot cm$	$f_{r,cal}/GHz$	μ_i	Damping factor, α
0.5	1.457	20	297.12	1.52	362	0.27
1	1.429	23	299.12	1.62	341	0.29
1.5	1.430	22	302.11	1.58	338	0.36
2	1.473	22	305.12	1.61	345	0.33
3	1.472	24	309.09	1.68	301	0.38
6	1.472	22	317.23	1.61	324	0.36
9	1.464	22	326.98	1.60	338	0.36
12	1.440	22	337.15	1.59	267	0.37

nm Al₂O₃ layer, the average saturation magnetization is 1.457 T that is larger than that (1.39 T) of the heavily boron doped single film that exhibits the best soft magnetic properties realized by tuning the boron concentration. The anisotropic field remains at $\sim 22 \times 79.6$ A/m and has no clear dependence on the insulating layer thickness. The induced anisotropy is dominant over the magnetocrystalline and magnetostrictive ones in the multilayer samples. The resistivity of the multilayer film increases from 195 to 337 $\mu\Omega \cdot cm$ by increasing the Al₂O₃ layer thickness. By increasing the thickness of Al₂O₃, the concentration of oxygen atoms will increase, the metal conduction mechanism will decrease and hence the resistivity will increase^[17]. The film resistivity with a 0.5 nm thick Al₂O₃ layer is 297.12 $\mu\Omega \cdot cm$, which is 1.5 times of the single layer value. Large resistivity will be favorable to reduce the eddy current loss in high frequency response. We may expect both electron tunneling and percolation through pinholes will dominate the vertical electron conduction when the insulating layer is ultra small^[35]. The average resistivity will be expected to have a maximum enhancement by a factor of 2 when the insulating layer is thick enough so that the top and bottom magnetic layers are totally isolated.

Complex permeability spectrum was measured for the multilayer films where well defined uniaxial anisotropy was developed^[36]. Figs. 6a~6f present the experimentally measured permeability spectra in zero bias field for the samples grown with different thicknesses of Al₂O₃ in the frequency range from 0.5 GHz to 4.0 GHz. Strong

ferromagnetic resonance characteristics are observed. The resonance frequency floats around 1.55 GHz and has weak dependence on the oxide layer thickness. These values are very close to the calculated resonance frequency $f_{r,cal}$ using M_s and H_k , as listed in Table 1. The real and imaginary permeability values decrease and the width of the imaginary permeability peak increases as the oxide layer gets thicker. Generally the existences of inhomogeneous domain orientation and damping are indicated^[37,38]. To quantitatively understand the effect of insulating layer onto the dynamic magnetic properties of the multilayer films, the complex permeability spectrum was further analyzed based on the Landu-Lifchitz-Gilbert (LLG) model that phenomenologically explains the dynamic magnetization behavior of magnetic materials^[39] by the equation:

$$\frac{dM}{dt} = -\gamma(M \times H) + \frac{\alpha}{M} M \times \frac{dM}{dt} \quad (3)$$

Solving the above LLG equation, we have the complex permeability spectrum approximated as^[25]

$$\mu_r(f) = 1 + \frac{\chi_o}{1 - (\frac{f}{f_r})^2 + j(\frac{2\alpha f}{f_r})} \quad (4)$$

$$f_r = \frac{\gamma}{2\pi} \mu_0 \sqrt{H_k M_s} \quad (5)$$

where f is the resonance frequency, χ_o is the static susceptibility, f_r is the operation frequency, $\gamma=1.78 \times 10^{11} (TS)^{-1}$ is the gyromagnetic ratio and α is the damping coefficient. We

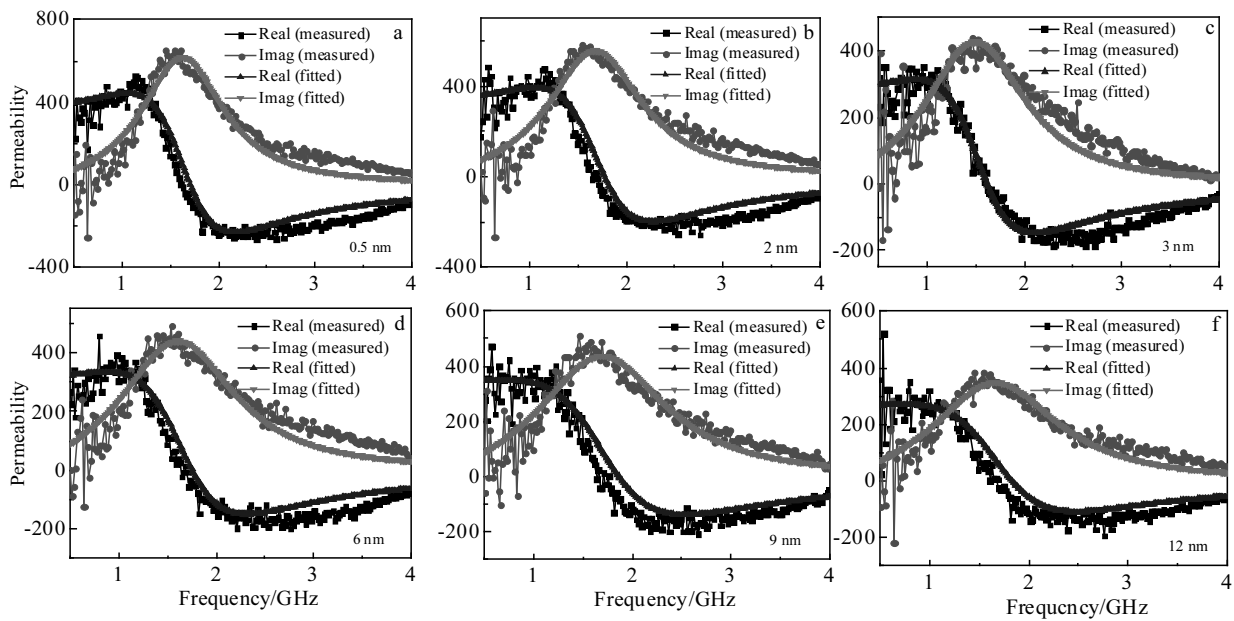


Fig.6 Permeability spectra of the sandwich structure FeGaB(25 nm)/Al₂O₃(x)/FeGaB(25 nm) at x=0.5 nm (a), x=2 nm (b), x=3 nm (c), x=6 nm (d), x=9 nm (e), and x=12 nm (f) (the dotted lines are the measured results and the solid lines are the fitting curves)

use Eq. (2) to fit the experimental permeability spectrum curves with M_s and H_k taken from the hysteresis loops. As shown by the solid lines in Figs. 6a~6f, the measured magnetic spectra could be well fitted by the theory.

The extracted damping parameter α as listed in Table 1 shows an increase with respect to the oxide layer thickness. It is worth noting that α is a phenomenological factor that includes the intrinsic and several extrinsic sources of damping. The intrinsic damping contributes to fundamental properties such as Zeeman transition while the issues like magnon scattering or local anisotropy dispersion contribute to external damping $\alpha_{int}^{[40]}$. In FeGaB/Al₂O₃/FeGaB multilayer structure, by increasing the thickness of Al₂O₃ there exist more defects and impurities in the film that contribute to the inhomogeneity of the multilayer films and consequently the damping factor increases^[41]. We may also expect that the reduction of the magnetostatic interaction across the thicker oxide layer effectively increases the anisotropy distribution, giving rise to an extrinsic damping. Table 1 also lists the initial permeability obtained from the fitting curve. We can see that the multilayer film developed here has the potential for high-frequency inductive applications.

3 Conclusions

1) FeGaB single layer and FeGaB/Al₂O₃/FeGaB multilayered structure are fabricated and we find that multilayered structure possess superior soft and high frequency microwave properties compared to FeGaB single layer, which can be adjusted by changing the thickness of Al₂O₃ layer.

2) A crystallographic change from <110> texture to

amorphous with Al₂O₃ thickness variation has no contribution to that particular change. By increasing the thickness of the Al₂O₃ layer, the values of resistivity ρ and damping factor α increase while the saturation magnetization $4\pi M_s$ decreases slightly.

3) A 0.5 nm thick Al₂O₃ insulating layer is thick enough to develop soft magnetic properties with coercivity 0.98×79.6 A/m, saturation magnetization 1.457 T, resistivity $297.12 \mu\Omega \cdot \text{cm}$ and less value of damping factor 0.27. The multilayer technique could be repeated to have thicker films or applied to other species of soft magnetic materials.

References

- 1 Estrine E C, Robbins W P, Maqableh M M et al. *Journal of Applied Physics*[J], 2013, 113(17): 17A937
- 2 Hamashima M, Saito C, Nakamura M et al. *Electronics & Communications in Japan*[J], 2012, 95(5): 1
- 3 Hui Y, Nan T X, Sun N X et al. *Micro Electro Mechanical Systems (MEMS)*[C]. Taiwan: IEEE, 2013
- 4 Basantkumar R R, Stadler B J, Robbins et al. *IEEE Transactions on Magnetics*[J], 2006, 42(10): 3102
- 5 Zhang X, Zhan Q, Dai G et al. *Journal of Applied Physics*[J], 2013, 113(17): 17A901
- 6 Lou J, Insignares R, Cai Z et al. *Applied Physics Letters*[J], 2007, 91(18): 182 504
- 7 Nakagawa S, Tanaka S, Suemitsu K et al. *Journal of Applied Physics*[J], 1996, 79(8): 5156
- 8 Platt C L, Minor M K, Klemmer T J et al. *IEEE Transactions on Magnetics*[J], 2001, 37(4): 2302
- 9 Hiramoto M, Matsukawa N, Sakakima H. *Journal of Magnetics Society of Japan*[J], 1999, 23(3): 867

- 10 Kim I, Kim J, Kim K H et al. *IEEE Transactions on Magnetics*[J], 2004, 40(4): 2706
- 11 Kobayashi T, Nakatani R, Ootomo S et al. *Journal of Applied Physics*[J], 1988, 64(6): 3157
- 12 Zhang Y, He P, Wang D et al. *Journal of Magnetism & Magnetic Materials*[J], 1994, 129(2-3): 351
- 13 Castaño F J, Stobiecki T, Gibbs M R J et al. *Thin Solid Films*[J], 1999, 348 (1-2): 233
- 14 Chopra H D, Yang D X, Chen P J et al. *Physical Review B*[J], 2000, 61(14): 9642
- 15 Wang S, Sun N, Yamaguchi M et al. *Nature*[J], 2000, 407(6801): 150
- 16 Cheng M, Lubitz P, Zheng Y et al. *Journal of Magnetism and Magnetic Materials*[J], 2004, 282: 109
- 17 Xu J, Dai B, Ren Y et al. *Journal of Materials Science: Materials in Electronics*[J], 2015, 26(5): 2931
- 18 Oliveira A J A de, Ortiz W A, Mosca D H et al. *Journal of Physics Condensed Matter*[J], 1998, 11(1): 47
- 19 Tomaz M A, Antel W J, O'Brien W L et al. *Phys Rev B*[J], 1997, 55(6): 3716
- 20 Xing X, Liu M, Li S et al. *IEEE Transactions on Magnetics*[J], 2011, 47(10): 3104
- 21 Nakagawa S, Suemitsu K, Naoe M. *Journal of Applied Physics*[J], 1997, 81(8): 3782
- 22 Naoe M, Miyamoto Y, Nakagawa S. *Journal of Applied Physics*[J], 1994, 75(10): 6525
- 23 Katori K, Hayashi K, Hayakawa M et al. *Applied Physics Letters*[J], 1989, 54(12): 1181
- 24 Yang X, Liu M, Peng B et al. *Applied Physics Letters*[J], 2015, 107(12): 173503
- 25 Liu Y, Chen L, Tan C et al. *Review of Scientific Instruments*[J], 2005, 76(6): 063 911
- 26 Ma Y G, Li X, Xie T et al. *Materials Science & Engineering B*[J], 2003, 103(3): 233
- 27 Ma Y G, Ong C K. *Journal of Physics D Applied Physics*[J], 2007, 40(40): 3286
- 28 Guittoum A, Bourzami A, Layadi A et al. *The European Physical Journal Applied Physics*[J], 2012, 58(2): 20 301
- 29 Jeon H J, Kim I, Kim J et al. *Journal of Magnetism & Magnetic Materials*[J], 2004, 272(2): 382
- 30 Zhang J, White R M. *Journal of Applied Physics*[J], 1996, 79(8): 5113
- 31 Herzer G. *IEEE Transactions on Magnetics*[J], 1990, 26(5): 1397
- 32 Morley N A, Javed A, Gibbs M R J. *Journal of Applied Physics*[J], 2009, 105(7): 07A912
- 33 Yang W, Lambeth D N, Laughlin D E. *Journal of Applied Physics*[J], 2000, 87(9): 6884
- 34 Javed A, Morley N A, Gibbs M R J. *Journal of Magnetism & Magnetic Materials*[J], 2009, 321(18): 2877
- 35 Meyerhofer D, Ochs S A. *Journal of Applied Physics*[J], 1963, 34(9): 2535
- 36 Ma Y G, Liu Y, Tan C Y et al. *Journal of Applied Physics*[J], 2006, 100(5): 054 307
- 37 Kuanr B K, Camley R E, Celinski Z. *Journal of Magnetism & Magnetic Materials*[J], 2005, 286: 276
- 38 Seemann K, Leiste H, Kovács A. *Journal of Magnetism & Magnetic Materials*[J], 2008, 320(13): 1952
- 39 Gilbert T L. *IEEE Transactions on Magnetics*[J], 2004, 40(6): 3443
- 40 Mircea D I, Clinton T W. *Applied Physics Letters*[J], 2007, 90(14): 142 504
- 41 Craus C B, Palasantzas G, Chezan A R et al. *Journal of Applied Physics*[J], 2005, 97(1): 013 904

FeGaB (25 nm)/Al₂O₃/FeGaB(25 nm)多层薄膜结构: 氧化铝(Al₂O₃)厚度变化对静态与动态磁性能的影响

Shahid Imran¹, 尹格², 元军², 马云贵², 何赛灵^{1,2,3}

(1. 华南师范大学 华师-浙大联合光子研究中心, 广东 广州 510006)

(2. 浙江大学 现代光学仪器国家重点实验室, 浙江 杭州 310058)

(3. 瑞典皇家理工学院, 瑞典 斯德哥尔摩 S-100 44)

摘要: 铁镓(FeGa)薄膜与其它软磁材料相比具有较大的磁致伸缩常数, 在设计集成磁性传感器芯片中具有独特的优势, 可通过采用非磁性掺杂和多层膜方法来控制这种合金薄膜的磁学与电学性能参数。在掺杂一定量硼(B)元素后, 厚度小于 30 nm 的 FeGa 薄膜顽力可以得到显著降低, 而对于较厚薄膜在插入超薄 Al₂O₃ 中间层后软磁性能可以得到同样程度显著改善, 同时饱和磁化(M_s)变化可忽略。对于我们制备的 FeGaB (25 nm)/Al₂O₃(0.5 nm)/FeGaB(25 nm)多层膜, 其易轴矫顽力可以小到 0.98 × 79.6 A/m, 电阻率与 50 nm 单层 FeGaB 膜相比增加了 1.5 倍, 同时具有吉赫兹高磁导率谱。样品微结构分析表明, 磁性颗粒结晶质量和物理尺寸的减小对软磁性改善起到重要作用, 另外也讨论分析了静磁相互作用和表面形貌对磁畴运动及矫顽力的影响。所发展的掺杂与多层膜混合方案来增强电磁性能的方法, 也可应用于其他类型的软磁材料系统。

关键词: 铁镓硼; 多层结构; 氧化铝; 软磁性能

作者简介: Shahid Imran, 男, 1977 年生, 博士生, 华南师范大学华师-浙大联合光子研究中心, 广东 广州 510006, 电话: 020-34728410, E-mail: shahidimran_77@yahoo.com